arXiv:1208.6542v1 [hep-ex] 31 Aug 2012

September 3, 2012

A Review of $\chi_{cJ}(1P)$ Decays at BESIII and CLEO-c

Ryan E. Mitchell

Department of Physics
Indiana University
Bloomington, Indiana 47405-7105

The latest results on $\chi_{cJ}(1P)$ decays from BESIII and CLEO-c are reviewed and compared to theoretical predictions. The experimental results use the final samples of $\chi_{cJ}(1P)$ decays from CLEO-c, obtained from 26 million $\psi(2S)$ decays, and the most recent samples from BESIII, from a starting sample of 106 million $\psi(2S)$ decays.

PRESENTED AT

The 5th International Workshop on Charm Physics
(Charm 2012)
Honolulu, Hawai'i, USA, May 14–17, 2012

1 Introduction

The $\chi_{cJ}(1P)$ states consist of a charm and an anticharm quark in a spin-1 (spin-aligned) state and with one unit of orbital angular momentum (P-wave) between them (Fig. 1). The total spin J is thus 0, 1, or 2. Since the χ_{cJ} are found abundantly in $\psi(2S)$ radiative decays, they can be most easily accessed at e^+e^- colliders where the $\psi(2S)$ can be directly produced. The χ_{cJ} decays covered in this review were collected by either the CLEO detector (starting with 26 million $\psi(2S)$ decays produced at the Cornell Electron Storage Ring (CESR)) or BESIII (starting with 106 million $\psi(2S)$ decays produced at the Beijing Electron Positron Collider (BEPCII)).

Decays of the χ_{cJ} can be used as important probes of strong force dynamics. The

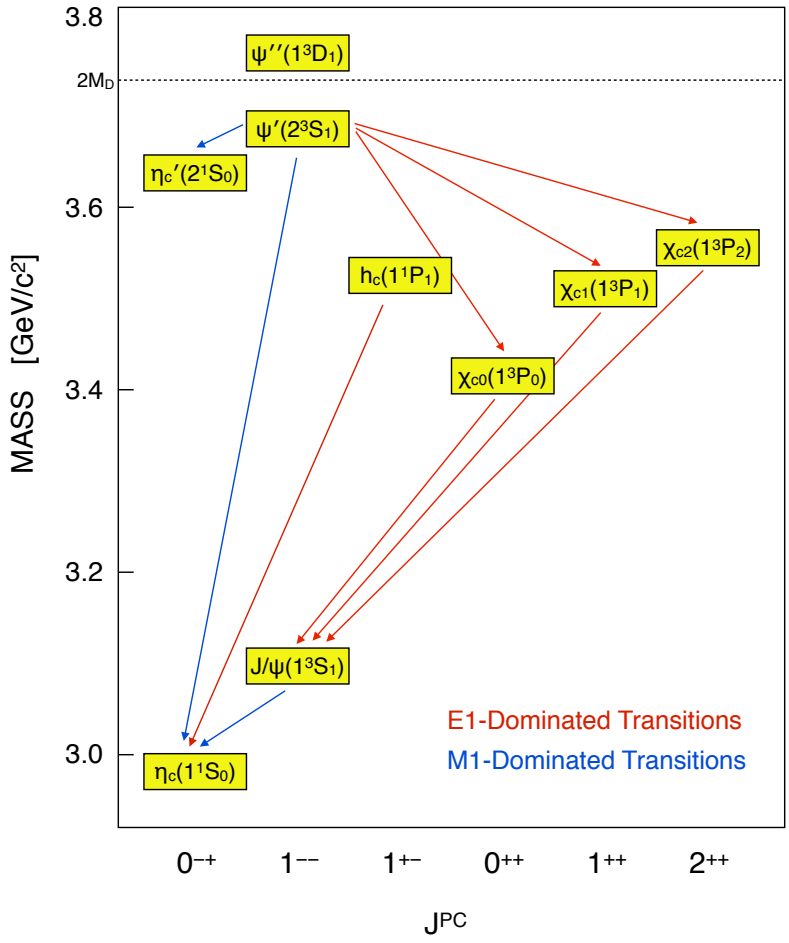


Figure 1: The charmonium system. The $\chi_{cJ}(1P)$ decays included in this review were obtained from $\psi(2S)$ radiative decays.

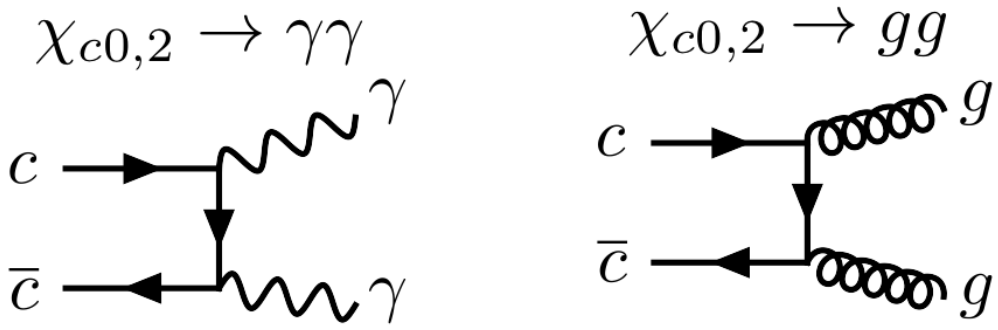


Figure 2: The lowest order perturbative QCD diagrams for electromagnetic (left) and strong (right) decays of the χ_{c0} and χ_{c2}.

mass is large enough that the decays can be treated perturbatively and the lowest order diagrams are quite simple (Fig. 2), consisting of only charm-anticharm quark annihilation into two photons (for the lowest order electromagnetic process) or into two gluons (for the lowest order strong process).

The lowest order diagram for $\chi_{c0,2} \to \gamma\gamma$ is pure QED, but the process is sensitive to QCD corrections. Since several theoretical uncertainties cancel in the ratio of χ_{c2} to χ_{c0} two-photon widths, the ratio $\mathcal{R}$, defined as:

$$\mathcal{R} = \frac{\Gamma(\chi_{c2} \to \gamma\gamma)}{\Gamma(\chi_{c0} \to \gamma\gamma)}, \tag{1}$$

is particularly important. Section 2 will cover a new BESIII result for $\mathcal{R}$ and the two-photon widths of the χ_{c0} and χ_{c2}.

The lowest order perturbative QCD diagrams for strong decays of the χ_{cJ} are shown in Fig. 3. The lowest order perturbative QCD diagrams do a poor job in many cases of predicting the patterns of χ_{cJ} decays. This has led some to consider the possibility that the χ_{cJ} exists partially in a color octet state, where gluons play a role as constituent particles. In this case, the simplest diagram is shown in the lower part of Fig. 3 and calculations have been performed using a Color Octet Model (COM) [1]. Sections 3 and 4 will review recent BESIII results for strong decays of the χ_{cJ}.

In addition to decay dynamics, exclusive χ_{cJ} decays are also a good source of light quark states, which is useful for both light quark meson and baryon spectroscopy. The rich set of final states available in χ_{cJ} decays allows one to isolate quantum numbers. Section 5 will review a recent analysis from CLEO, where an amplitude analysis was performed on the decays $\chi_{c1} \to \eta^{(\prime)}\pi^+\pi^-$ and evidence was found for a light quark state with exotic quantum numbers decaying to $\eta'\pi$.

While CLEO concluded data-taking in 2008, the BESIII experiment continues to collect additional data in the charmonium region. We thus expect further improvements in our understanding of χ_{cJ} decays in the near future.

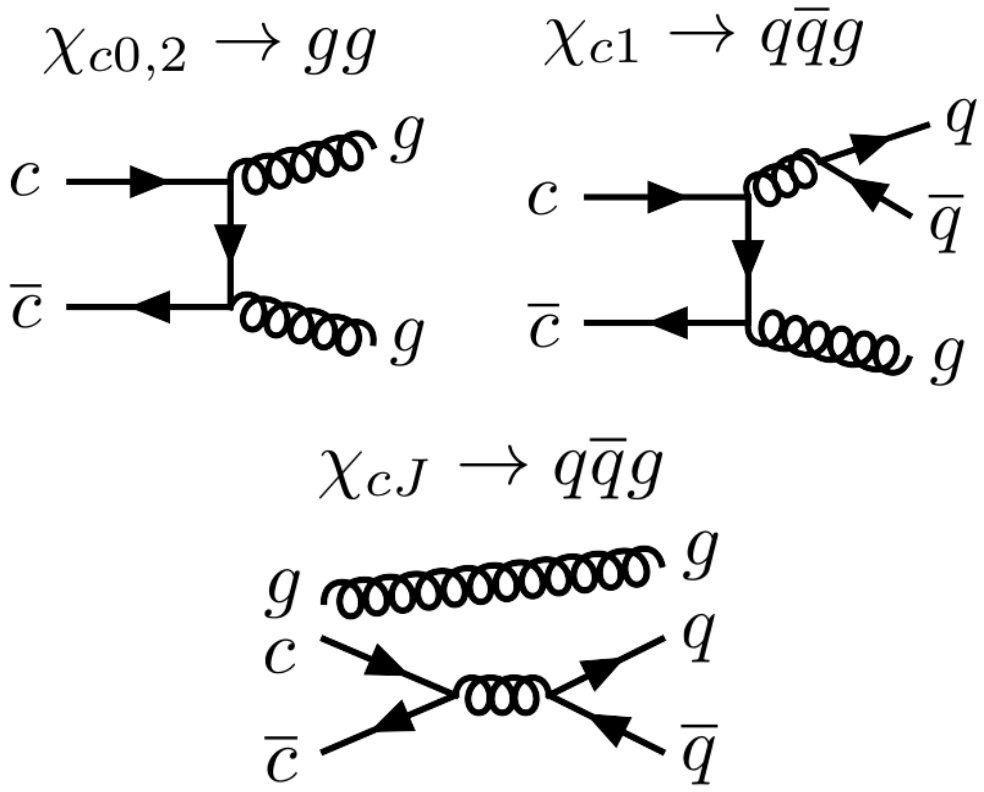
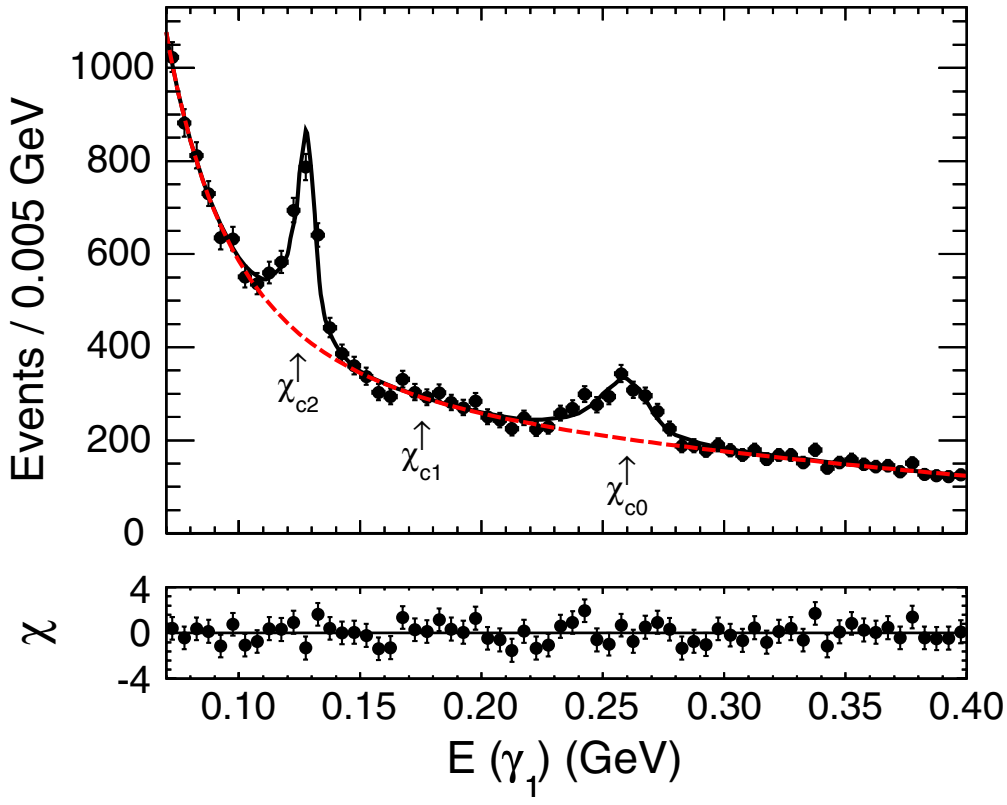


Figure 3: The lowest order perturbative QCD diagrams for strong decays of the χ_{cJ}. The bottom figure assumes the initial χ_{cJ} is in a color octet state.

2 Electromagnetic Decays

As mentioned in the introduction, the lowest-order diagrams for $\chi_{c0,2} \to \gamma\gamma$ are purely QED, but the process is sensitive to higher-order QCD effects, such as radiative or relativistic corrections. To lowest order in QED, the ratio of two-photon widths of the χ_{c0} and χ_{c2}, $\mathcal{R}$, defined in Eqn. 1, is $4/15 \approx 0.27$. With QCD corrections, the predicted value ranges from 0.09 to 0.36 depending on the model [2, 3]. Thus, precision measurements of $\mathcal{R}$ are important for arbitrating between models.

BESIII recently published new measurements of χ_{c0} and χ_{c2} two-photon widths (and thus $\mathcal{R}$) [4], using the 3-photon process $\psi(2S) \to \gamma\chi_{c0,2}; \chi_{c0,2} \to \gamma\gamma$. Results are shown in Fig. 4. The energy of the lowest-energy photon (called γ_1 in Fig. 4) was used to tag the χ_{c0} or χ_{c2}. The shape of the background, which is dominated by non-$\psi(2S)$ QED processes, was derived from data taken off-resonance at 3650 MeV. The signal shapes were taken from a control sample of $\psi(2S) \to \gamma\chi_{c0,2}; \chi_{c0,2} \to K^+K^-$.



Quantity	χ_{c0}	χ_{c2}
$\mathcal{B}_1 \times \mathcal{B}_2 \times 10^5$	$2.17 \pm 0.17 \pm 0.12$	$2.81 \pm 0.17 \pm 0.15$
$\mathcal{B}_2 \times 10^4$	$2.24 \pm 0.19 \pm 0.12 \pm 0.08$	$3.21 \pm 0.18 \pm 0.17 \pm 0.13$
$\Gamma_{\gamma\gamma}$ (keV)	$2.33 \pm 0.20 \pm 0.13 \pm 0.17$	$0.63 \pm 0.04 \pm 0.04 \pm 0.04$
$\mathcal{R}$	$0.271 \pm 0.029 \pm 0.013 \pm 0.027$	

Figure 4: Precision measurements of $\mathcal{B}_1(\psi(2S) \to \gamma\chi_{c0,2}) \times \mathcal{B}_2(\chi_{c0,2} \to \gamma\gamma)$ from BESIII [4]. The figures show the energy distribution of the photon from the $\psi(2S)$ to $\chi_{c0,2}$ transition and the χ distribution resulting from the fit. The table shows the results, where $\Gamma_{\gamma\gamma}$ is the two-photon widths of the $\chi_{c0,2}$ and $\mathcal{R}$ is the ratio of the widths. The first errors are statistical, the second systematic, and the third from PDG inputs (for $\mathcal{B}_1$ and the full widths of the χ_{c0} and χ_{c2}).

The final results are also listed in Fig. 4, where $\mathcal{B}_1 \equiv \mathcal{B}(\psi(2S) \to \gamma\chi_{c0,2})$ and $\mathcal{B}_2 \equiv \mathcal{B}(\chi_{c0,2} \to \gamma\gamma)$. For normalization, $\mathcal{B}_1$ and the full widths of the χ_{c0} and χ_{c2} were taken from the PDG [5]. The final result for $\mathcal{R}$, perhaps surprisingly, is consistent with the lowest-order QED calculation.

3 Strong Decays to Mesons

The decays of the χ_{cJ} into two vector mesons ($J^{PC} = 1^{--}$), for example $\chi_{cJ} \to \omega\omega, \omega\phi, \phi\phi$, have a number of interesting features. First, from perturbative QCD, one would expect the branching fractions to be smaller than 10^{-3}. Second, the helicity selection rule predicts the decays of the χ_{c1} to two vector mesons to be suppressed. And finally, the decays $\chi_{cJ} \to \phi\phi, \omega\omega$ are only singly OZI-suppressed (as are all charmonium decays), while the decays $\chi_{cJ} \to \omega\phi$ are doubly OZI-suppressed. This can be seen in the diagrams shown in Fig. 5.

BESIII published new results on $\chi_{cJ} \to \omega\omega, \phi\phi, \omega\phi$ in 2011 [6] that address these issues. The results are shown in Fig. 6, where the small peaking backgrounds have been estimated from ω or ϕ sidebands. First, the branching fractions are on the order of 10^{-3}, somewhat higher than one would expect from perturbative QCD. Second, there are substantial rates for the χ_{c1} decays, which appears to contradict expectations from the helicity selection rule. Finally, BESIII made the first observations of the doubly OZI-suppressed $\chi_{cJ} \to \omega\phi$ decays, with branching fractions roughly an order of magnitude down from the singly OZI-suppressed decays. The resulting numbers are shown in Fig. 7.

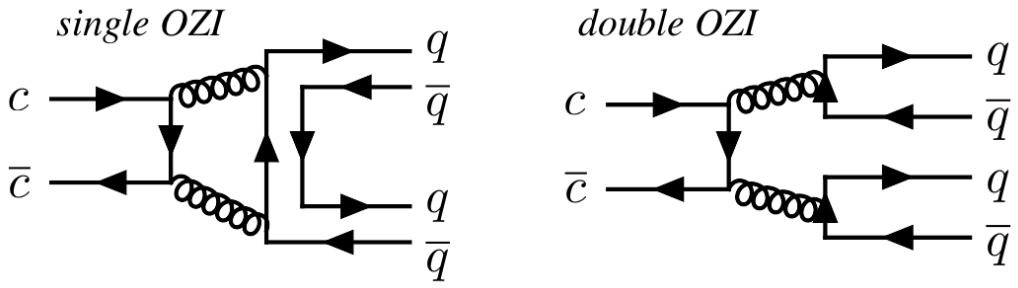


Figure 5: Diagrams for single and double OZI-violating decays of the χ_{cJ} to two vector states (ω, ϕ). The lowest order diagrams for the decays $\chi_{cJ} \to \omega\phi$ are double OZI-violating.

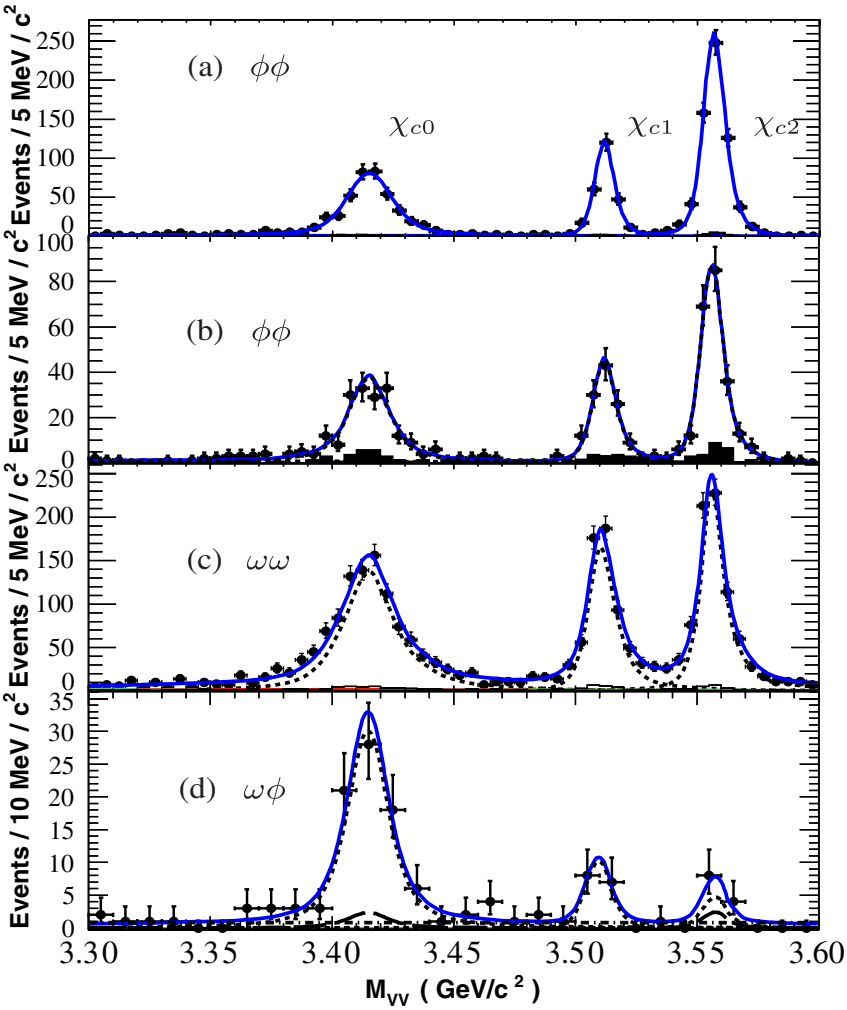


Figure 6: Measurements of χ_{cJ} decays to (a,b) $\phi\phi$, (c) $\omega\omega$, and (d) $\omega\phi$ from BESIII [6]. In (b), one of the ϕ decays to $\pi^+\pi^-\pi^0$. In all other cases the ϕ decays to K^+K^-.

Mode	$N_{\rm net}$	ϵ (%)	$\mathcal{B}(\times 10^{-4})$
$\chi_{c0} \to \phi\phi$	433 ± 23	22.4	$7.8 \pm 0.4 \pm 0.8$
$\chi_{c1} \to \phi\phi$	254 ± 17	26.4	$4.1 \pm 0.3 \pm 0.4$
$\chi_{c2} \to \phi\phi$	630 ± 26	26.1	$10.7 \pm 0.4 \pm 1.1$
$\to 2(K^+K^-)$			
$\chi_{c0} \to \phi\phi$	179 ± 16	12.8	$9.2 \pm 0.7 \pm 1.0$
$\chi_{c1} \to \phi\phi$	112 ± 12	15.3	$5.0 \pm 0.5 \pm 0.6$
$\chi_{c2} \to \phi\phi$	219 ± 16	14.9	$10.7 \pm 0.7 \pm 1.2$
$\to K^+K^-\pi^+\pi^-\pi^0$			
Combined:			
$\chi_{c0} \to \phi\phi$	$\cdots$	$\cdots$	$8.0 \pm 0.3 \pm 0.8$
$\chi_{c1} \to \phi\phi$	$\cdots$	$\cdots$	$4.4 \pm 0.3 \pm 0.5$
$\chi_{c2} \to \phi\phi$	$\cdots$	$\cdots$	$10.7 \pm 0.3 \pm 1.2$
$\chi_{c0} \to \omega\omega$	991 ± 38	13.1	$9.5 \pm 0.3 \pm 1.1$
$\chi_{c1} \to \omega\omega$	597 ± 29	13.2	$6.0 \pm 0.3 \pm 0.7$
$\chi_{c2} \to \omega\omega$	762 ± 31	11.9	$8.9 \pm 0.3 \pm 1.1$
$\to 2(\pi^+\pi^-\pi^0)$			
$\chi_{c0} \to \omega\phi$	76 ± 11	14.7	$1.2 \pm 0.1 \pm 0.2$
$\chi_{c1} \to \omega\phi$	15 ± 4	16.2	$0.22 \pm 0.06 \pm 0.02$
$\chi_{c2} \to \omega\phi$	<13	15.7	<0.2
$\to K^+K^-\pi^+\pi^-\pi^0$			

Figure 7: The number of observed events ($N_{\rm net}$), the efficiencies (ϵ), and the branching fractions ($\mathcal{B}$) for the decay modes listed in the first column. The results are from BESIII [6].

4 Strong Decays to Baryons

The simplest baryon decays of the χ_{cJ}, namely $\chi_{c1} \to p\overline{p}$ and $\chi_{c2} \to p\overline{p}$, have long presented a theoretical challenge. While the perturbative QCD calculations, assuming the χ_{cJ} is in a color singlet state, predict $\mathcal{B}(\chi_{c1} \to p\overline{p}) = 0.29 \times 10^{-5}$ and $\mathcal{B}(\chi_{c2} \to p\overline{p}) = 0.84 \times 10^{-5}$, the experimental measurements are an order of magnitude larger. Furthermore, the decay $\chi_{c0} \to p\overline{p}$ (and χ_{c0} decays to baryon anti-baryon pairs in general) should be suppressed in perturbative QCD by the "helicity selection rule," which links the final state hadrons to the helicities of the intermediate gluons. But experimentally, substantial χ_{c0} decay rates have been found.

To address the discrepancy between theory and experiment in χ_{c1} and χ_{c2} $p\overline{p}$ decays, a "color octet model" (COM) was devised, which allows the χ_{cJ} to have a color octet component in which there is a valence gluon [1]. This model was able to bring the theoretical $p\overline{p}$ branching fractions into alignment with experiment, but still underestimated other baryon-antibaryon decays such as $\Lambda\overline{\Lambda}$. A comparison of COM predictions and experimental measurements from the PDG are shown in Fig. 8.

Inspired by these COM predictions, there has recently been a series of analyses from BESIII looking at χ_{cJ} decays to baryon pairs [7, 8]. The new results from BESIII are also listed in Fig. 8.

The first BESIII measurements are of χ_{cJ} decays to $\Lambda\overline{\Lambda}$, $\Sigma^0\overline{\Sigma}^0$, and $\Sigma^+\overline{\Sigma}^-$. The signals are shown in Fig. 9 and the χ_{c1} and χ_{c2} branching fractions are listed in Fig. 8.

	χ_{c1} Decays (units of 10^{-5})			χ_{c2} Decays (units of 10^{-5})		
Decay Mode	COM	PDG	NEW from BESIII	COM	PDG	NEW from BESIII
$p\overline{p}$	6.5	7.3 ± 0.4	–	7.8	7.2 ± 0.4	–
$n\overline{n}$	6.5	–	–	7.8	–	–
$\Lambda\overline{\Lambda}$	3.9	11.8 ± 1.9	$12.2 \pm 1.1 \pm 1.1$	3.5	18.6 ± 2.7	$20.8 \pm 1.6 \pm 2.2$
$\Sigma^0\overline{\Sigma}^0$	3.3	< 4	$3.8 \pm 1.0 \pm 0.5$	5.0	< 8	$4.0 \pm 1.1 \pm 0.4$
$\Sigma^+\overline{\Sigma}^-$	3.3	< 6	$5.4 \pm 1.5 \pm 0.4$	5.0	< 7	$4.9 \pm 1.9 \pm 0.6$
$\Xi^0\overline{\Xi}^0$	2.5	< 6	–	3.7	< 11	–
$\Xi^-\overline{\Xi}^+$	2.5	8.4 ± 2.3	–	3.7	15.5 ± 3.5	–
$\Delta\overline{\Delta}$	3.9	–	–	6.3	–	–
$\Sigma^{+*}(1385)\overline{\Sigma}^{-*}(1385)$	2.1	–	$4.4 \pm 2.5 \pm 0.6$ (< 10)	3.6	–	$7.9 \pm 4.0 \pm 0.9$ (< 17)
$\Sigma^{-*}(1385)\overline{\Sigma}^{+*}(1385)$	2.1	–	< 5.7	3.6	–	< 8.5
$\Xi^*\overline{\Xi}^*$	1.1	–	–	2.1	–	–
$\Lambda(1520)\overline{\Lambda}(1520)$	–	–	< 8.6	–	–	51 ± 13

Figure 8: The Color Octet Model (COM) [1] predictions, the Particle Data Group (PDG) [5] values, and new BESIII measurements [7, 8] of branching fractions of χ_{c1} and χ_{c2} decays to various di-baryon final states. All branching fractions are in units of 10^{-5}.

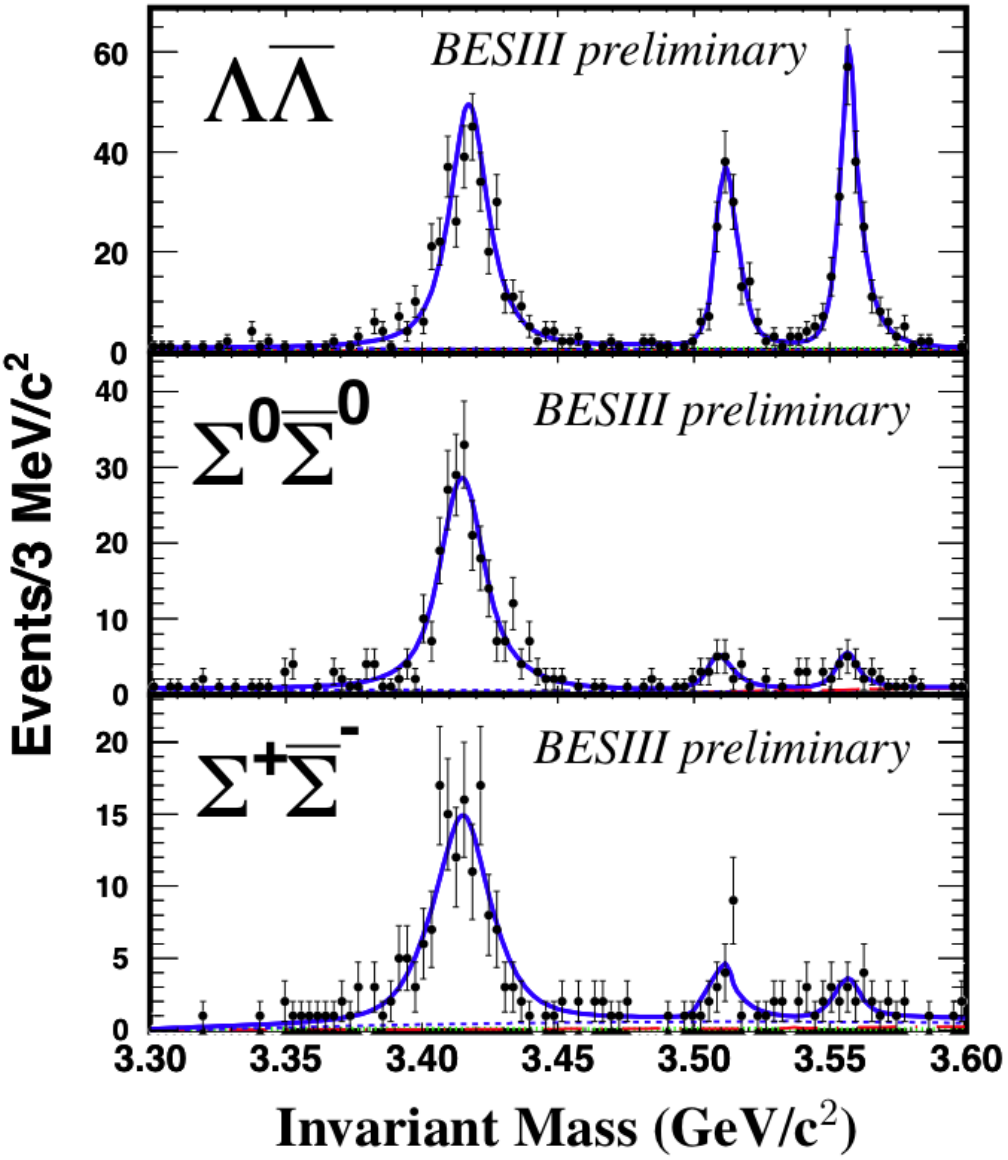


Figure 9: Preliminary measurements of branching fractions of χ_{cJ} decays to $\Lambda\overline{\Lambda}$, $\Sigma^0\overline{\Sigma}^0$, and $\Sigma^+\overline{\Sigma}^-$ from BESIII.

The $\Lambda\overline{\Lambda}$ branching fractions are still significantly larger than the COM predictions, while the $\Sigma\overline{\Sigma}$ decays appear to be consistent, although with large statistical errors. Interestingly, the χ_{c0} branching fractions, which are predicted to be suppressed by the helicity selection rule, are far larger than those of the $\chi_{c1,2}$. The preliminary results from BESIII for the χ_{c0} decays are $\mathcal{B}(\chi_{c0} \to \Lambda\overline{\Lambda}) = (33.3 \pm 2.0 \pm 2.6) \times 10^{-5}$, $\mathcal{B}(\chi_{c0} \to$

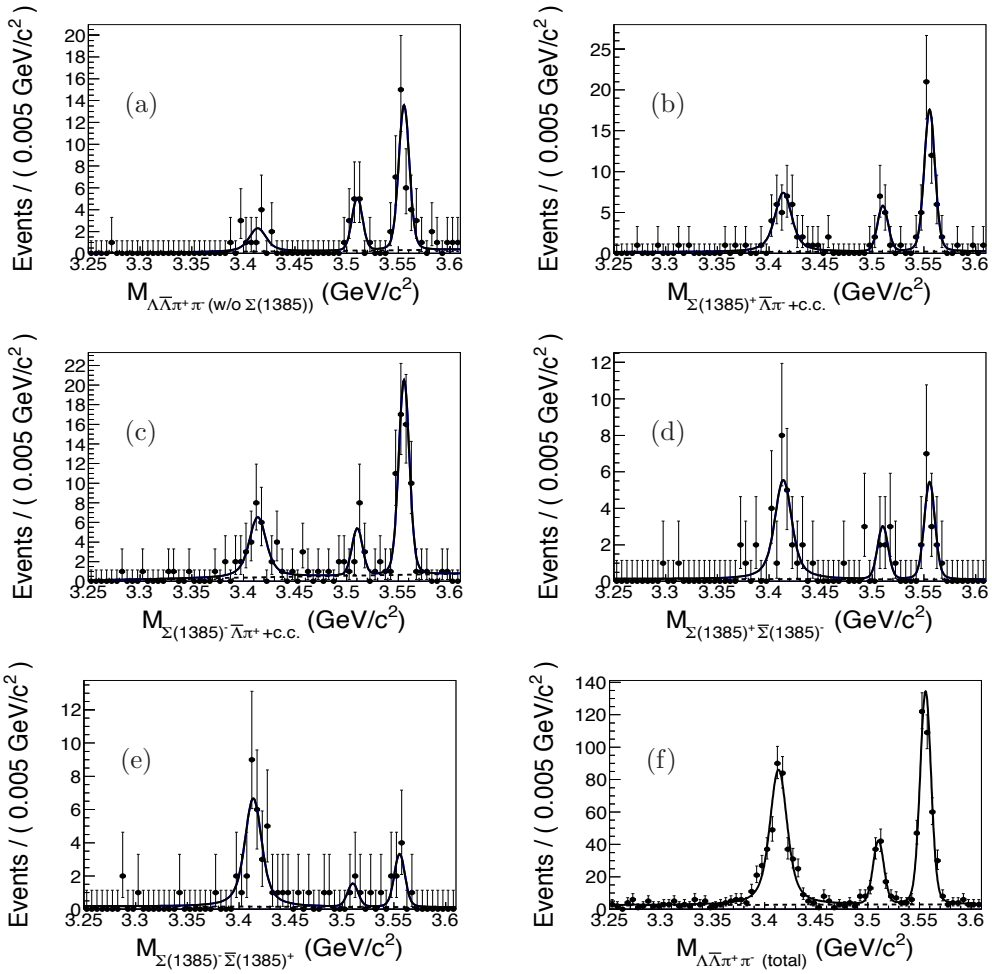


Figure 10: BESIII measurements of χ_{cJ} yields in decays to $\Lambda\overline{\Lambda}\pi^+\pi^-$ in regions corresponding to (a) no $\Sigma(1385)$, (b) the $\Sigma(1385)^+$, (c) the $\Sigma(1385)^-$, (d) the $\Sigma(1385)^+$ and $\overline{\Sigma}(1385)^-$, (e) the $\Sigma(1385)^-$ and $\overline{\Sigma}(1385)^+$, and (f) all regions [7].

$\Sigma^0\overline{\Sigma}^0) = (47.8 \pm 3.4 \pm 3.8) \times 10^{-5}$, and $\mathcal{B}(\chi_{c0} \to \Sigma^+\overline{\Sigma}^-) = (45.4 \pm 4.2 \pm 2.5) \times 10^{-5}$.

The second BESIII measurements [7] consist of χ_{cJ} decays to $\Lambda\overline{\Lambda}\pi^+\pi^-$ and all of the intermediate processes that can be produced with the $\Sigma(1385)$. Of particular interest for comparison with the COM are the $\chi_{c1,2}$ decays to $\Sigma(1385)^+\overline{\Sigma}(1385)^-$ and $\Sigma(1385)^-\overline{\Sigma}(1385)^+$. The χ_{cJ} peaks for various regions of $\Lambda\overline{\Lambda}\pi^+\pi^-$ sub-masses are shown in Fig. 10. Since the $\Sigma(1385)$ is fairly wide, and overlaps significantly with $\Lambda\overline{\Lambda}\pi^+\pi^-$ phase space, the various branching fractions (with different combinations of $\Sigma(1385)$) were extracted using a matrix of efficiencies and overlaps determined from signal Monte Carlo. The results are listed in Fig. 11. The χ_{c1} and χ_{c2} decays are consistent with the COM predictions (within large statistical errors). But again, the

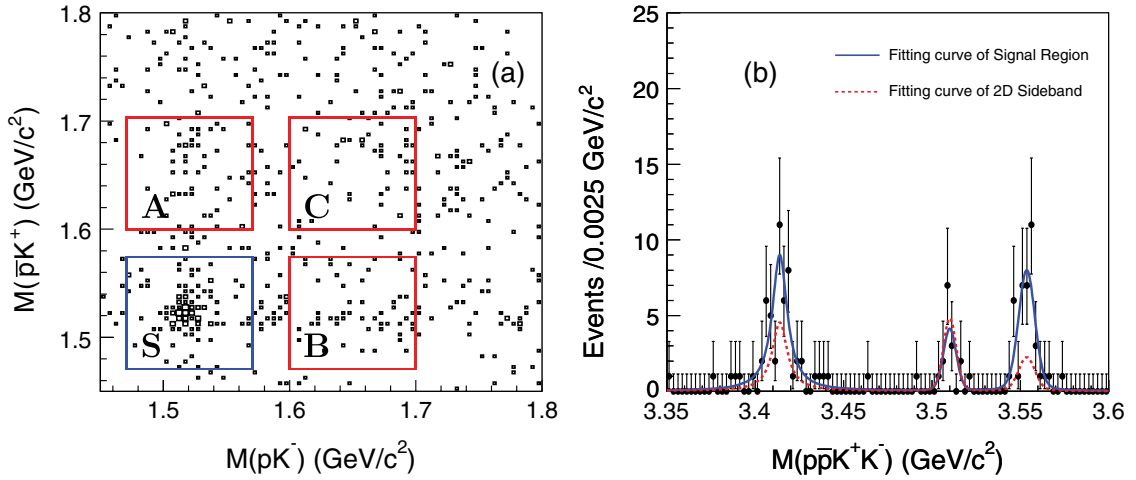
χ_{cJ} decay mode	χ_{c0}			χ_{c1}			χ_{c2}		
	$\mathcal{B}$	UL	S	$\mathcal{B}$	UL	S	$\mathcal{B}$	UL	S
$\Lambda\bar{\Lambda}\pi^+\pi^-$ (w/o $\Sigma(1385)$)	28.6±12.6±2.7	<54	2.2	26.2±5.5±3.3		4.8	71.8±14.5±8.2		6.4
$\Sigma(1385)^+\bar{\Lambda}\pi^- + c.c.$	34.8±13.2±3.4	<55	2.2		<14	0.3	23.6±11.8±2.7	<42	1.7
$\Sigma(1385)^-\bar{\Lambda}\pi^+ + c.c.$	24.6±12.7±2.4	<50	1.6		<14	0.0	37.8±11.8±4.4	<61	2.6
$\Sigma(1385)^+\bar{\Sigma}(1385)^-$	16.4±5.7±1.6		3.1	4.4±2.5±0.6	<10	1.9	7.9±4.0±0.9	<17	2.0
$\Sigma(1385)^-\bar{\Sigma}(1385)^+$	23.5±6.2±2.3		4.3		<5.7	0.9		<8.5	0.0
$\Lambda\bar{\Lambda}\pi^+\pi^-$(total)	119.0±6.4±11.4		> 10	31.1±3.4±3.9		> 10	137.0±7.6±15.7		> 10

Figure 11: BESIII measurements of χ_{cJ} branching fractions to $\Lambda\overline{\Lambda}\pi^+\pi^-$ and various combinations of internal $\Sigma(1385)$ decays [7]. Branching fractions ($\mathcal{B}$) are in units of 10^{-5} and upper limits (UL) are at 90% confidence level. The significance of each channel is given in the S column.

χ_{c0} decays appear to be dominant.

Finally, BESIII has also measured the decays $\chi_{cJ} \to \Lambda(1520)\overline{\Lambda}(1520)$ using the final state $K^+K^-p\overline{p}$. Signal and sideband regions were defined in $M(\overline{p}K^+)$ and $M(pK^-)$ and a simultaneous fit was performed to these regions, as shown in Fig. 12. The final results are also listed in Fig. 12. Perhaps surprisingly, the rates for χ_{c0} and χ_{c2} decays to $\Lambda(1520)\overline{\Lambda}(1520)$ are as large as those to $\Lambda\overline{\Lambda}$ (which were already larger than the COM predictions).

As can be seen in Fig 8, the COM is successful (within experimental uncertainties) in describing many χ_{c1} and χ_{c2} decays into baryons and anti-baryons. The $\Lambda\overline{\Lambda}$ channel is the notable exception. Since the BESIII measurements were inspired by the COM, the focus has been on comparisons between experiment and that model. Note that other models exist, however, and can be found extensively reviewed in [9].



	χ_{c0}	χ_{c1}	χ_{c2}
$\mathcal{B}(\chi_{cJ} \to p\bar{p}K^+K^-)$ (10^{-4})	$1.24 \pm 0.20 \pm 0.18$	$1.35 \pm 0.15 \pm 0.19$	$2.08 \pm 0.19 \pm 0.30$
$\mathcal{B}(\chi_{cJ} \to \bar{p}K^+\Lambda(1520) + \text{c.c.})$ (10^{-4})	$3.00 \pm 0.58 \pm 0.50$	$1.81 \pm 0.38 \pm 0.28$	$3.06 \pm 0.50 \pm 0.54$
$\mathcal{B}(\chi_{cJ} \to \Lambda(1520)\bar{\Lambda}(1520))$ (10^{-4})	$3.18 \pm 1.11 \pm 0.53$	<1.00	$5.05 \pm 1.29 \pm 0.93$
$\mathcal{B}(\chi_{cJ} \to p\bar{p}\phi)$ (10^{-5})	$6.12 \pm 1.18 \pm 0.86$	<1.82	$3.04 \pm 0.85 \pm 0.43$

Figure 12: BESIII measurements of $\chi_{cJ} \to p\bar{p}K^+K^-$ and its submodes involving $\Lambda(1520) \to pK^-$, $\overline{\Lambda}(1520) \to \bar{p}K^+$, and $\phi \to K^+K^-$. The upper plots show the selection of the $\Lambda(1520)\overline{\Lambda}(1520)$ signal region (left) and the resulting χ_{cJ} peaks (right). The solid (blue) line is a fit in the signal region and the dotted (red) line is a fit in the sidebands. The table lists the resulting branching fractions.

5 Light Meson Spectroscopy in χ_{cJ} Decays

Decays of the χ_{cJ} are not only important for the study of the strong force through the dynamics of their decays, but they also serve as a source of light quark states. The large number of available final states, and the fact the initial state can have $J = 0, 1, 2$, depending on the χ_{cJ} state, allows one to optimize searches for light quark mesons with specific quantum numbers. The decays $\chi_{c1} \to \eta\pi^+\pi^-$ and $\chi_{c1} \to \eta'\pi^+\pi^-$, for example, are an ideal place to search for resonances with exotic $J^{PC} = 1^{-+}$ quantum numbers decaying to $\eta\pi$ or $\eta'\pi$. The possible resonances produced in $\chi_{c1} \to \eta^{(\prime)}\pi^+\pi^-$ decays are listed in Fig. 13. Here the only allowed S-wave decay of the χ_{c1} goes through the exotic π_1 state, which in turn decays to $\eta^{(\prime)}\pi$.

χ_{c1} Decay Mode	L	Isobar J^{PC}
$a_0\pi;\ a_0 \to \eta^{(\prime)}\pi$	P	0^{++}
$\pi_1\pi;\ \pi_1 \to \eta^{(\prime)}\pi$	S, D	1^{-+}
$a_2\pi;\ a_2 \to \eta^{(\prime)}\pi$	P, F	2^{++}
$a_4\pi;\ a_4 \to \eta^{(\prime)}\pi$	F, H	4^{++}
$f_0\eta^{(\prime)};\ f_0 \to \pi\pi$	P	0^{++}
$f_2\eta^{(\prime)};\ f_2 \to \pi\pi$	P, F	2^{++}
$f_4\eta^{(\prime)};\ f_4 \to \pi\pi$	F, H	4^{++}

Figure 13: A list of allowed decays of the χ_{c1} that result in the final state $\eta^{(\prime)}\pi^+\pi^-$, the angular momentum ($L$) of the initial χ_{c1} decay, and the J^{PC} of the intermediate state. Notice that the decay through the exotic π_1 state is the only allowed S-wave decay and thus could be enhanced relative to other decay modes.

The CLEO Collaboration has recently published an amplitude analysis of the decays $\chi_{c1} \to \eta^{(\prime)}\pi^+\pi^-$ [10]. Clean samples of the χ_{c1}, shown in Fig. 14, were obtained from 26 million $\psi(2S)$ decays. An amplitude analysis was then performed using the amplitudes listed in Fig. 13. Breit-Wigner distributions were used to parameterize most resonance decays, while a Flatte distribution was used for $a_0(980)$ decays, and a phenomenological distribution taken from $\pi\pi$ scattering data was used for the $\pi\pi$ S-wave (called f_0 in Fig. 13). Projections of the fit results are shown in Fig. 15 and the results are listed in Fig. 16.

In the $\chi_{c1} \to \eta'\pi^+\pi^-$ channel, CLEO found evidence for an exotic π_1 state decaying to $\eta'\pi$, which is consistent with previous claims of a $\pi_1(1600)$ state produced in other

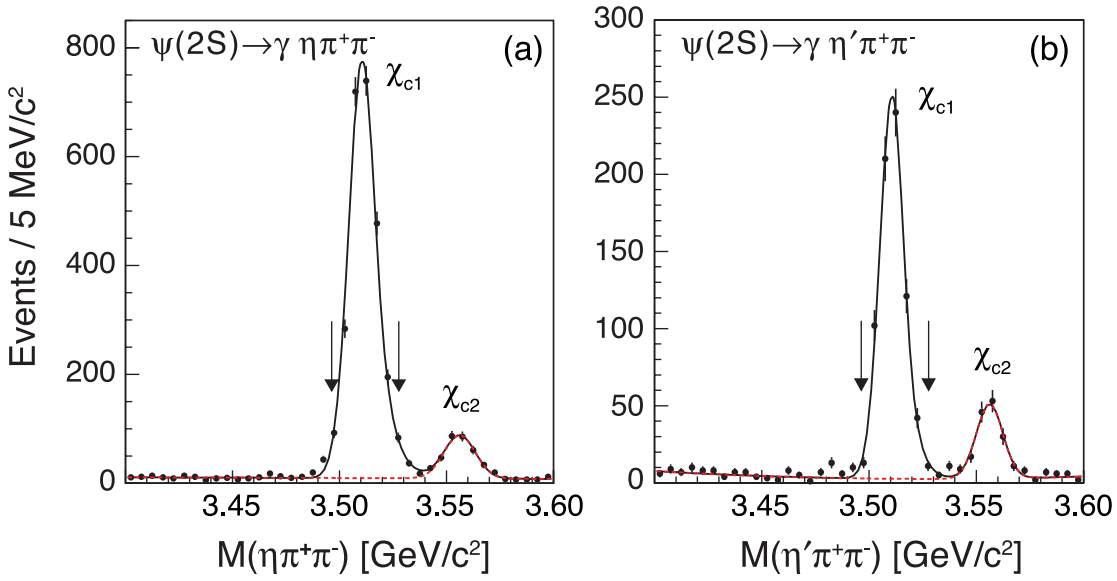


Figure 14: The selection of χ_{c1} decays to $\eta\pi^+\pi^-$ (left) and $\eta'\pi^+\pi^-$ (right) from CLEO [10]. The signal purities are estimated to be 97.5% and 94.6%, respectively.

production mechanisms [11]. This is the first evidence of a light quark meson with exotic quantum numbers in a charmonium decay, and opens many new possibilities for other amplitude analyses of χ_{cJ} decays into other final states.

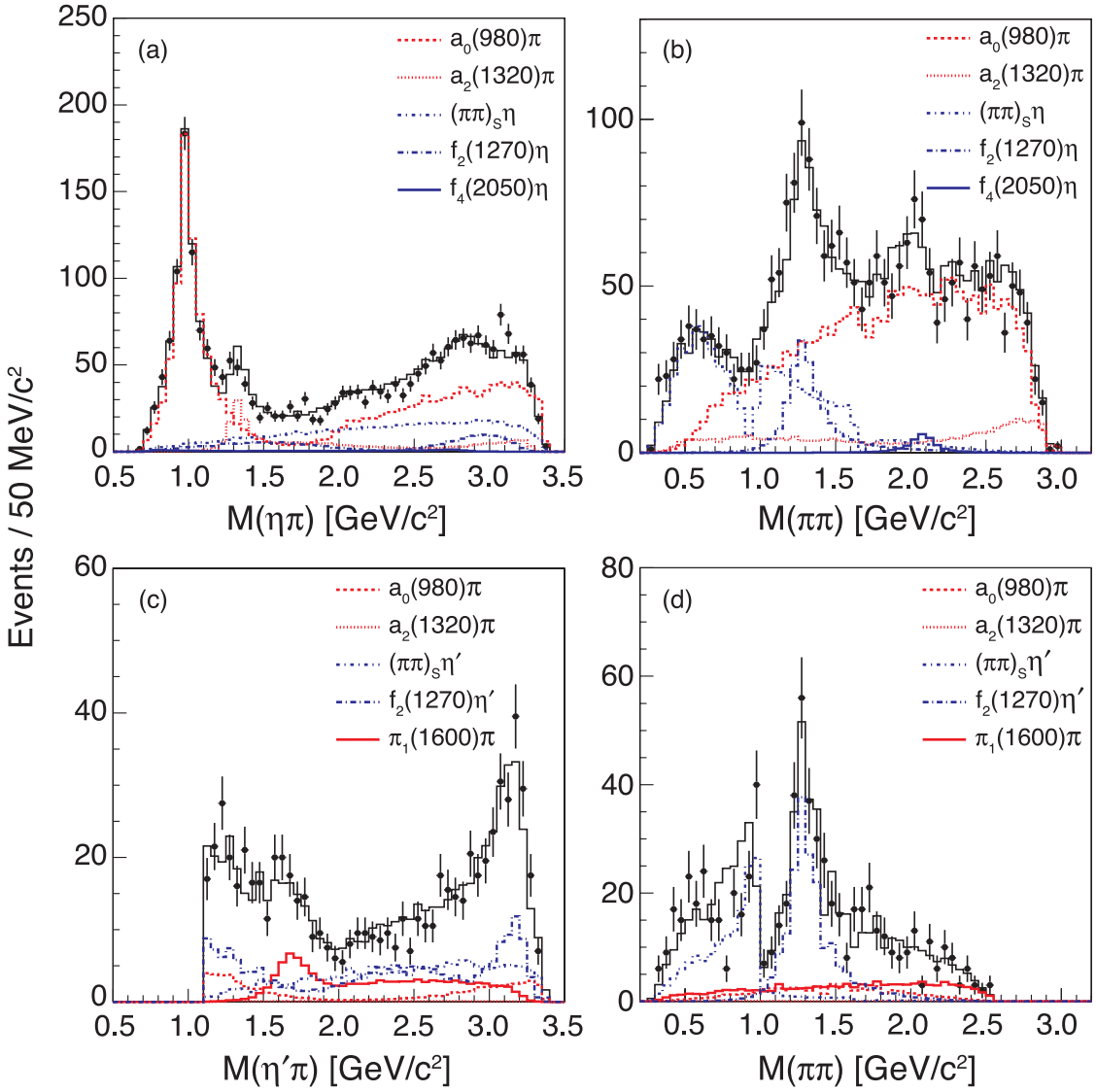


Figure 15: The fit results for $\chi_{c1} \to \eta\pi^+\pi^-$ (top) and $\chi_{c1} \to \eta'\pi^+\pi^-$ (bottom) from CLEO [10]. The points are data and the solid black line is the total fit result. The other lines show contributions from individual amplitudes. The exotic π_1 signal decaying to $\eta'\pi$ can be seen in the lower left.

χ_{c1} Decay Mode	$\mathcal{F}$ [%]	$\mathcal{B}(\chi_{c1} \to \eta^{(\prime)}\pi^+\pi^-) \times \mathcal{F}$ [10^{-3}]	N_σ
$\eta\pi^+\pi^-$	$\cdots$	$4.97 \pm 0.08 \pm 0.21 \pm 0.22$	$\cdots$
$a_0(980)\pi$	$66.2 \pm 1.2 \pm 1.1$	$3.29 \pm 0.09 \pm 0.14 \pm 0.15$	>10
$a_2(1320)\pi$	$9.8 \pm 0.8 \pm 1.0$	$0.49 \pm 0.04 \pm 0.05 \pm 0.02$	9.7
$(\pi^+\pi^-)_S\eta$	$22.5 \pm 1.3 \pm 2.5$	$1.12 \pm 0.06 \pm 0.13 \pm 0.05$	>10
$S^0_{\pi\pi}\eta$	$12.1 \pm 1.7 \pm 5.6$	$0.60 \pm 0.08 \pm 0.28 \pm 0.03$	>10
$S^1_{\pi\pi}\eta$	$3.4 \pm 0.9 \pm 1.5$	$0.17 \pm 0.05 \pm 0.07 \pm 0.01$	6.0
$S_{KK}\eta$	$3.1 \pm 0.6 \pm 0.4$	$0.15 \pm 0.03 \pm 0.02 \pm 0.01$	9.4
$f_2(1270)\eta$	$7.4 \pm 0.8 \pm 0.6$	$0.37 \pm 0.04 \pm 0.04 \pm 0.02$	>10
$f_4(2050)\eta$	$1.0 \pm 0.3 \pm 0.3$	$0.05 \pm 0.01 \pm 0.02 \pm 0.00$	5.2
$^*\pi_1(1600)\pi$	$\cdots$	<0.031	0.7
$\eta'\pi^+\pi^-$	$\cdots$	$1.90 \pm 0.07 \pm 0.08 \pm 0.09$	$\cdots$
$a_0(980)\pi$	$11.0 \pm 2.3 \pm 1.8$	$0.21 \pm 0.04 \pm 0.04 \pm 0.01$	8.4
$a_2(1320)\pi$	$0.4 \pm 0.5 \pm 0.6$	<0.031	1.4
$(\pi^+\pi^-)_S\eta$	$21.6 \pm 2.7 \pm 1.2$	$0.41 \pm 0.05 \pm 0.03 \pm 0.02$	10.2
$S^0_{\pi\pi}\eta'$	$7.0 \pm 2.2 \pm 2.3$	$0.13 \pm 0.04 \pm 0.04 \pm 0.01$	6.6
$S_{KK}\eta'$	$8.4 \pm 1.5 \pm 1.3$	$0.16 \pm 0.03 \pm 0.02 \pm 0.01$	7.5
$f_2(1270)\eta'$	$27.0 \pm 2.9 \pm 1.7$	$0.51 \pm 0.06 \pm 0.04 \pm 0.03$	>10
$^*f_4(2050)\eta'$	$\cdots$	<0.010	0.4
$\pi_1(1600)\pi$	$15.1 \pm 2.7 \pm 3.2$	$0.29 \pm 0.05 \pm 0.06 \pm 0.01$	7.2

Figure 16: Results from the CLEO amplitude analyses of $\chi_{c1} \to \eta^{(\prime)}\pi^+\pi^-$ showing the fit fractions ($\mathcal{F}$) of different submodes, the branching fraction of $\chi_{c1} \to \eta^{(\prime)}\pi^+\pi^-$ times the fit fractions ($\mathcal{B} \times \mathcal{F}$), and the significance of each fit component (N_σ) [10]. The first errors are statistical, the second systematic, and the third, where applicable, are from the external measurement of $\mathcal{B}(\psi(2S) \to \gamma\chi_{c1})$.

6 Conclusion

While data taking has concluded at CLEO, and no new χ_{cJ} analyses are anticipated, BESIII continues to collect data in the charmonium region. The BESIII results presented here are based on 106 million $\psi(2S)$ decays, but more statistics are expected. With larger statistics, we expect to learn more about strong decay dynamics and perform more searches for light quark states in χ_{cJ} decays.

References

[1] S. M. H. Wong, Eur. Phys. J. C **14**, 643 (2000) [hep-ph/9903236].

[2] S. N. Gupta, J. M. Johnson and W. W. Repko, Phys. Rev. D **54**, 2075 (1996) [hep-ph/9606349].

[3] S. Godfrey and N. Isgur, Phys. Rev. D **32**, 189 (1985).

[4] M. Ablikim *et al.* [BESIII Collaboration], Phys. Rev. D **85**, 112008 (2012) [arXiv:1205.4284 [hep-ex]].

[5] K. Nakamura *et al.* [Particle Data Group Collaboration], J. Phys. G G **37**, 075021 (2010).

[6] M. Ablikim, M. N. Achasov, L. An, Q. An, Z. H. An, J. Z. Bai, R. Baldini and Y. Ban *et al.*, Phys. Rev. Lett. **107**, 092001 (2011) [arXiv:1104.5068 [hep-ex]].

[7] [BESIII Collaboration], arXiv:1207.5646 [hep-ex[.

[8] M. Ablikim [BESIII Collaboration], Phys. Rev. D **83**, 112009 (2011) [arXiv:1103.2661 [hep-ex]].

[9] N. Brambilla, S. Eidelman, B. K. Heltsley, R. Vogt, G. T. Bodwin, E. Eichten, A. D. Frawley and A. B. Meyer *et al.*, Eur. Phys. J. C **71**, 1534 (2011) [arXiv:1010.5827 [hep-ph]].

[10] G. S. Adams *et al.* [CLEO Collaboration], Phys. Rev. D **84**, 112009 (2011) [arXiv:1109.5843 [hep-ex]].

[11] J. Beringer *et al.* [Particle Data Group Collaboration], Phys. Rev. D **86**, 010001 (2012).